Structural Engineering and Mechanics, *Vol. 71, No. 2 (2019) 197-210*
DOI: https://doi.org/10.12989/sem.2019.71.2.197

Probabilistic assessment on buckling behavior of sandwich panel: - A radial basis function approach

R.R. Kumar*, K.M. Pandey and S. Dey

Mechanical Engineering Department, National Institute of Technology Silchar, India

(Received October 27, 2018, Revised March 26, 2019, Accepted March 31, 2019)

Abstract. Probabilistic buckling behavior of sandwich panel considering random system parameters using a radial basis function (RBF) approach is presented in this paper. The random system properties result in an uncertain response of the sandwich structure. The buckling load of laminated sandwich panel is obtained by employing higher-order-zigzag theory (HOZT) coupled with RBF and probabilistic finite element (FE) model. The in-plane displacement variation of core as well as facesheet is considered to be cubic while transverse displacement is considered to be quadratic within the core and constant in the facesheets. Individual and combined stochasticity in all elemental input parameters (like facesheets thickness, ply-orientation angle, core thickness and properties of material) are considered to know the effect of different degree of stochasticity, ply- orientation angle, boundary conditions, core thickness, number of laminates, and material properties on global response of the structure. In order to achieve the computational efficiency, RBF model is employed as a surrogate to the original finite element model. The stiffness matrix of global response is stored in a single array using skyline technique and simultaneous iteration technique is used to solve the stochastic buckling equations.

Keywords: sandwich panel; probabilistic buckling behavior; radial basis function; random properties; higher order zigzag theory

1. Introduction

In general, a sandwich panel is made up of facesheet at outer layers and the core inserted in between them wherein the facesheets are fabricated with stiff and strong materials but of relatively lower thickness than that of light and thicker core. It is not necessary for the core as well as facesheet material of a sandwich panel to be homogeneous in nature. Broad application area of the sandwich structure is portrayed in Figure 1. In a sandwich panel, a core is having low strength and high energy absorption capability whereas facesheet is having high strength and ductility (Caliskan and Apalak (2017)). Recently, interest in the sandwich panel was observed to be concentrated on the core of the lattice structure (Bart-Smith *et al*. (2001), Fan *et al*. (2010), Wang *et al*. (2010)). Stretching causes the deformation in members of a truss, presented in lattice structured core.

Sandwich panel with lattice core exhibits greater specific strength and stiffness, but it gets crumbled in compression due to buckling (may be elastic or inelastic) of truss member when it is sufficiently slender (Deshpande and Fleck (2001, 2003)). Thus sandwich panels with lattice core are undesirable in energy absorbing applications, as a result of which foam cores are used in sandwich panels where energy absorbing criterion is of prime interest because of their higher energy absorbability (Rizov *et al*. (2005)). To increase the energy absorption capability, in addition to top and bottom facesheet, one additional facesheet is used in between core (Al-Shamary *et al*. (2016)). The energy absorption capability and penetration threshold can be improved by using multi-walled carbon nanotubes (MWCNTs) in the manufacturing of foam core (Taraghi and Fereidoon (2016)). Buckling analysis of FGM sandwich plate is carried out in a hygrothermal environment by sobhy (2016) whereas it is carried out for FG facesheet and soft core conical sandwich shell by seidi *et al*. (2015). Moita *et al*. (2015) presented FEM based buckling analysis of sandwich panel wherein it is stated that buckling analysis of soft core sandwich panel could not be carried out by using equivalent single layer (ESL) models. Kolahachi (2017) presented refined zig-zag theory (RZT) which do not require shear correction factor for buckling, deflection and frequency prediction. Applicability of higher order Zig-Zag theory (HOZT) is checked for both soft core and hard core sandwich plates by Nguyen *et al*. (2015). Sandwich plates with CNT reinforced nanocomposite facesheet are studied for their buckling response by Moradi-Dastjerdi and Malek-Mohammadi (2017). Global buckling response of circular sandwich plates is presented (both analytically and numerically) by Blandzi *et al*. (2018). Global buckling response and wrinkling of facesheet are carried out by Khalili *et al*. (2015) and Hohe J. (2015). Kahya (2016) proposed N-layered beam element having 3N+7 degree of freedom for buckling analysis wherein delamination between the layers is eliminated. Bi-axial buckling analysis is investigated for soft core sandwich plate using improved HOZT by Kheirikhah *et al*. (2012). Thermal buckling load has been

*Corresponding author, Ph.D.
E-mail: ravi@rs.mech.student.nits.ac.in

ISSN: 1225-4568 (Print), 1598-6217 (Online)

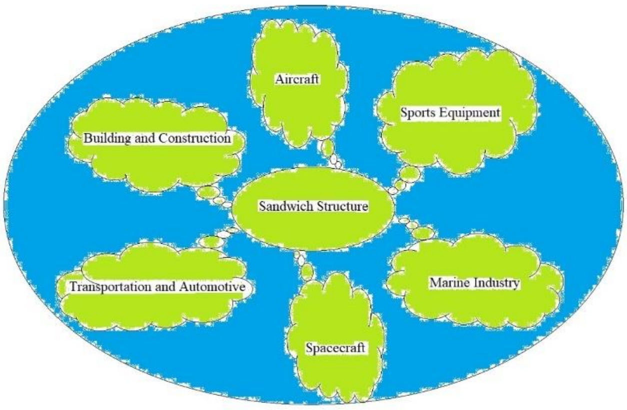

Fig. 1 Sectors where sandwich structures are in use

estimated by Shia and Kuo (2004) using higher order triangular plate element of 36 degrees of freedom whereas thermal post-buckling behavior for laminated shell panel has been reported by Panda and Singh (2013). Golchi *et al.* (2018) reported the critical temperature for buckling of a stiffened conical shell made up of FGM. Gupta and Talha (2018) considered porosity and geometric imperfections (initial) in FGM plates to study their stability behavior. Kacar and Yildirim (2016) have considered helical spring made up of composites for buckling and frequency response under initial static axial force and moment. Alamatian and Goshik (2017) calculated the buckling load by an efficient modified dynamic relaxation method. Influence of scattering in material properties are considered for buckling and vibration analysis of composite plate by Wang *et al.* (2011). The Variational principle is used by Muradova *et al.* (2009) to model the von karman plate for buckling loads. Xin *et al.* (2011) presented that, there is a significant effect of crack length and crack orientation on buckling, vibration and dynamic stability of a cylindrical shell. The analytical approach is used to calculate the buckling load for elastic medium embedded Euler column by Yayli (2018). Several researchers (Mohammadimehr *et al.* (2017), Sekkal *et al.* (2017), Poortabib and Maghsoudi (2014), Elmossouess *et al.* (2017), Tounsi *et al.* (2016), El-Haina *et al.* (2017)) has conducted deterministic buckling analysis of sandwich and FG plates and beams. Some researchers studied probabilistic analysis for buckling response of sandwich plates (Li *et al.* (2016), Lal *et al.* (2012), Lal at al. (2015), Ikeda *et al.* (2009)) whereas some researchers (Karsh *et al.* (2018a), Karsh *et al.* (2018b), Karsh *et al.* (2018c), Karsh *et al.* (2019), Kumar *et al.* (2019) and Mukhopadhyay *et al.* (2018)) carried out surrogate based stochastic analysis.

After a thorough review of the literature, a few research works are observed on the probabilistic assessment of buckling response for the sandwich panel. Most of the research article is based on the deterministic analysis which is non-judicial to consider for design and analysis of sophisticated structure because of the unavoidable source uncertainties present in the system it is impossible to manufacture as per the nominal (deterministic) value of design data. Few researchers focused on stochastic analysis wherein they used time-consuming conventional Monte Carlo simulation approach for probabilistic characterization of buckling response of the structure. Some researchers also focused on a surrogate based stochastic analysis of composites, but no research is carried out for buckling load of sandwich panels using RBF surrogate model coupled finite element approach. Conventional MCS approach becomes more inefficient due to randomness in a large number of input parameters (60 in present analysis). In the present study, nine noded isoparametric bending elements are used in FE formulation for stochastic buckling analysis, and layer-wise bottom-up approach is employed in a random environment for surrogate-based finite element iterations. Two types of uncertainties (material and geometric) are considered in the present analysis. Here buckling load is estimated for the individual as well as combined variation of input parameters. The sandwich panel under consideration is having linear zigzag lamina of different slopes for which stochastic C^0 finite element formulation is implemented. The Monte Carlo simulation (MCS) in conjunction to FE method is employed to map the comprehensive probabilistic response of the structure, but it requires ten-thousands (10,000) of expensive and time-consuming FE simulations to be carried out. Here Finite element-RBF coupled simulation approach is adopted to diminish this lacuna and be benefitted of the capabilities of MCS simultaneously. The FE model of sandwich panels is not completely replaced by the RBF model although the RBF is employed to complement the ability of FE model. The novelty of the present study lies in the integration of stochastic buckling analysis with the constructed efficient radial basis function (RBF) model employed for sandwich panels. The RBF in conjunction with finite element analysis can be applied to all structures (in the present case it is laminated sandwich composite panel) to achieve computational efficiency without affecting the accuracy. It is to be noted that the analytical approach is not possible at all in case of the complex structure as it leads to intensive mathematical equations although the FE approach is suitable for analyzing such complex structure (sandwich panel with facesheet of laminated composite) as the purpose for which it is developed. The finite element approach is also having a drawback of high computational time which is taken care by coupling RBF with FE method. First of all, the FE simulations are carried out to choose optimal design points. These design points are used to form the RBF surrogate model and thereby MCS is carried out by using a constructed RBF model. Hence, the complete stochastic description of the buckling load can be obtained by using the computationally efficient RBF based MCS method.

This article is hereafter demonstrated as follows: the mathematical formulation for stochastic buckling load of sandwich panels is presented in section 2; Section 3 demonstrates the RBF based surrogate modelling, RBF-FE based stochastic buckling analysis is presented in section 4; Deterministic validation of Finite element (FE) code and RBF surrogate model validation with original FE model along with stochastic results considering combined as well as individual variation of input parameters are demonstrated in section 5; and finally the outlook and conclusion of this paper is presented in section 6.

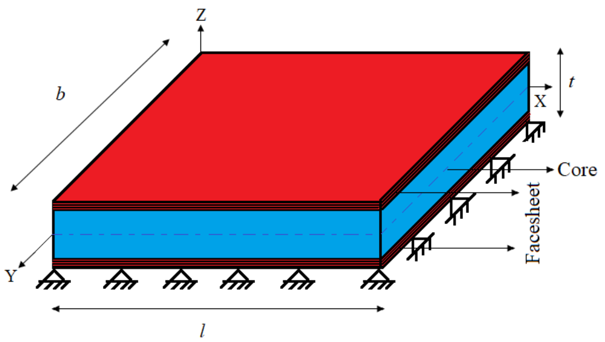

Fig. 2 Simply-supported laminated sandwich panel

2. Mathematical formulation for stochastic buckling analysis of sandwich panels

Let us consider a simply supported sandwich panel (Figure 1) having facesheet made up of laminated ('n' number of thin lamina) composite panel. For the ease of calculation, normal to the reference plane (deformed) of sandwich panel is assumed to remain straight. Let's assume $\{Q_k(\varpi)\}$ as transformed rigidity matrix of k-th lamina, $\{\sigma(\varpi)\}$ as stress vector and $\{\varepsilon(\varpi)\}$ as the strain vector where ϖ represents the stochasticity. If 'θ' is the fiber orientation angle of orthotropic lamina of k-th layer in reference to structural axes system (X-Y-Z) then, as per Kirchhoff hypothesis the stress-strain relationship (Chalak *et al.* (2015)) for sandwich panel can be presented as $\{\sigma(\varpi)\} = \{Q_k(\varpi)\}\{\varepsilon(\varpi)\}$

$$\begin{Bmatrix}\sigma_{xx}(\varpi)\\ \sigma_{yy}(\varpi)\\ \sigma_{zz}(\varpi)\\ \tau_{xy}(\varpi)\\ \tau_{xz}(\varpi)\\ \tau_{yz}(\varpi)\end{Bmatrix}=\begin{bmatrix}Q_{11}(\varpi) & Q_{12}(\varpi) & Q_{13}(\varpi) & Q_{14}(\varpi) & 0 & 0\\ Q_{21}(\varpi) & Q_{22}(\varpi) & Q_{23}(\varpi) & Q_{24}(\varpi) & 0 & 0\\ Q_{31}(\varpi) & Q_{32}(\varpi) & Q_{33}(\varpi) & Q_{34}(\varpi) & 0 & 0\\ Q_{41}(\varpi) & Q_{42}(\varpi) & Q_{43}(\varpi) & Q_{44}(\varpi) & 0 & 0\\ 0 & 0 & 0 & 0 & Q_{55}(\varpi) & Q_{56}(\varpi)\\ 0 & 0 & 0 & 0 & Q_{65}(\varpi) & Q_{66}(\varpi)\end{bmatrix}_K\begin{Bmatrix}\varepsilon_{xx}(\varpi)\\ \varepsilon_{yy}(\varpi)\\ \varepsilon_{zz}(\varpi)\\ \gamma_{xy}(\varpi)\\ \gamma_{xz}(\varpi)\\ \gamma_{yz}(\varpi)\end{Bmatrix} \quad (1)$$

If t_c is the core thickness, t_f is the facesheet thickness and t is the total thickness then it can be written as $t = t_c + 2t_f$. Let's assume facesheet rotation in x-z plane as Φ_x and core rotation in x-z plane as Ψ_x.

If u_0 is the in-plane displacement of a point on mid-surface in X-direction, v_0 is the in-plane displacement of a point on mid-surface in Y-direction, θ_x is the rotation of normal to mid-plane about Y axis, θ_y is the rotation of normal to mid-plane about X axis, n_u is the number of upper layer, n_l is the number of lower layer then in-plane displacement field as shown in figure 3 can be expressed as

$$U_X = u_0 + z\theta_x + \sum_{k=1}^{n_u-1}\left(z-z_k^u\right)(\varpi)H\left(z-z_k^u\right)\beta_{xu}^k + \sum_{m=1}^{n_l-1}\left(z-z_m^l\right)(\varpi)H\left(-z+z_m^l\right)\beta_{xl}^m + \alpha_x z^2 + \psi_x z^3 \quad (2)$$

$$V_X = v_0 + z\theta_y + \sum_{k=1}^{n_u-1}\left(z-z_k^u\right)(\varpi)H\left(z-z_k^u\right)\beta_{yu}^k + \sum_{m=1}^{n_l-1}\left(z-z_m^l\right)(\varpi)H\left(-z+z_m^l\right)\beta_{yl}^m + \alpha_y z^2 + \psi_y z^3 \quad (3)$$

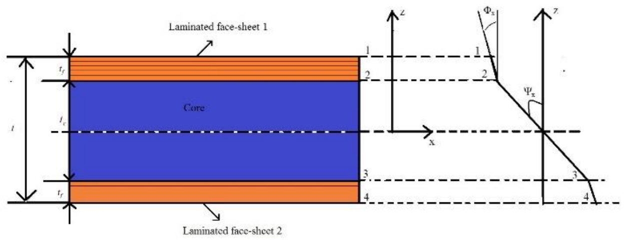

Fig. 3 In-plane displacement of Sandwich panel

Here, $H(z-z_k^u)$ and $H(-z+z_m^l)$ represents the Heaviside step functions whereas coefficients of higher order unknowns are indicated as α_x, α_y, Ψ_x. Ψ_y. and slope of k-th and m-th layer is represented by $\beta_{xu}^k, \beta_{yu}^m, \beta_{xi}^k, \beta_{yu}^m$.

If $w_l(\varpi)$, $w_o(\varpi)$, $w_u(\varpi)$ are transverse displacement values for lower, middle and upper layer of the core, respectively then equation 4, 5, and 6 represents transverse displacement value for upper layer facesheet, core and lower layer facesheet respectively.

$$W(\varpi) = w_u(\varpi) \quad (4)$$

$$W(\varpi) = \frac{z(z+t_l)}{t_u(t_u+t_l)}w_u(\varpi) + \frac{(z+t_l)(t_u-z)}{t_l t_u}w_0(\varpi) + \frac{z(t_u-z)}{-t_l(t_u+t_l)}w_l(\varpi) \quad (5)$$

$$W(\varpi) = w_l(\varpi) \quad (6)$$

Nine noded isoparametric elements with eleven degree of freedom (u_o, v_o, w_o, θ_x, θ_y, u_u, v_u, w_u, u_l, v_l, and w_l) per node are considered for finite element analysis. The node transformation matrix $[T_{node}(\varpi)]$ and element transformation matrix $[T_{element}(\varpi)]$ are expressed in eq. (7) and eq. (8) respectively

$$[T_{node}(\varpi)] = \begin{bmatrix} m & -n & 0 & 0 & 0 & 0 & 0 & 0 & 0 & 0 & 0\\ n & m & 0 & 0 & 0 & 0 & 0 & 0 & 0 & 0 & 0\\ 0 & 0 & 1 & 0 & 0 & 0 & 0 & 0 & 0 & 0 & 0\\ 0 & 0 & 0 & m & -n & 0 & 0 & 0 & 0 & 0 & 0\\ 0 & 0 & 0 & n & m & 0 & 0 & 0 & 0 & 0 & 0\\ 0 & 0 & 0 & 0 & 0 & m & -n & 0 & 0 & 0 & 0\\ 0 & 0 & 0 & 0 & 0 & n & m & 0 & 0 & 0 & 0\\ 0 & 0 & 0 & 0 & 0 & 0 & 0 & 1 & 0 & 0 & 0\\ 0 & 0 & 0 & 0 & 0 & 0 & 0 & 0 & m & -n & 0\\ 0 & 0 & 0 & 0 & 0 & 0 & 0 & 0 & n & m & 0\\ 0 & 0 & 0 & 0 & 0 & 0 & 0 & 0 & 0 & 0 & 1 \end{bmatrix} \quad (7)$$

$$[T_{element}(\varpi)] = \begin{bmatrix} [T_n(\varpi)] & 0 & 0 & 0 & 0 & 0 & 0 & 0 & 0 & 0 & 0\\ 0 & [T_n(\varpi)] & 0 & 0 & 0 & 0 & 0 & 0 & 0 & 0 & 0\\ 0 & 0 & [T_n(\varpi)] & 0 & 0 & 0 & 0 & 0 & 0 & 0 & 0\\ 0 & 0 & 0 & [T_n(\varpi)] & 0 & 0 & 0 & 0 & 0 & 0 & 0\\ 0 & 0 & 0 & 0 & [T_n(\varpi)] & 0 & 0 & 0 & 0 & 0 & 0\\ 0 & 0 & 0 & 0 & 0 & [T_n(\varpi)] & 0 & 0 & 0 & 0 & 0\\ 0 & 0 & 0 & 0 & 0 & 0 & [T_n(\varpi)] & 0 & 0 & 0 & 0\\ 0 & 0 & 0 & 0 & 0 & 0 & 0 & [T_n(\varpi)] & 0 & 0 & 0\\ 0 & 0 & 0 & 0 & 0 & 0 & 0 & 0 & [T_n(\varpi)] & 0 & 0\\ 0 & 0 & 0 & 0 & 0 & 0 & 0 & 0 & 0 & [T_n(\varpi)] & 0\\ 0 & 0 & 0 & 0 & 0 & 0 & 0 & 0 & 0 & 0 & [T_n(\varpi)] \end{bmatrix} \quad (8)$$

In case of structural deformation, relation for strain-displacement can be written as

$$\{\bar{\varepsilon}(\varpi)\} = \begin{bmatrix} \dfrac{\partial U(\varpi)}{\partial x} \dfrac{\partial V(\varpi)}{\partial y} \dfrac{\partial W(\varpi)}{\partial z} \dfrac{\partial U(\varpi)}{\partial x} \\ +\dfrac{\partial V(\varpi)}{\partial y} \dfrac{\partial U(\varpi)}{\partial z} + \dfrac{\partial W(\varpi)}{\partial x} \dfrac{\partial V(\varpi)}{\partial z} + \dfrac{\partial W(\varpi)}{\partial x} \end{bmatrix} \quad (9)$$

i.e. $\bar{\varepsilon}\{(\varpi)\} = [H(\varpi)]\{\varepsilon(\varpi)\}$ Here, unit step function is represented by $[H]$.

Transverse shear stress is assumed to be continuous in between two layers and it is assumed to be zero at bottom and top surface. If $u = u_l$, $v = v_l$ for bottom layer of panel, $u = u_u$, $v = v_u$ for top layer of panel then $\alpha_x, \alpha_y, \psi_x, \psi_y, \beta_{xu}^k, \beta_{yu}^m, \beta_{xl}^k, \beta_{yl}^m, (\partial w_u/\partial x), (\partial w_l/\partial x), (\partial w_u/\partial y), (\partial w_l/\partial y)$ can be written in terms of displacements u_o, v_o, θ_x, θ_y, u_u, u_l, v_u, v_l, as:

$$\{A\}=[C]\ \{\beta\} \quad (10)$$

Here,

$$\{A\}=\{\alpha_x\ \psi_x\ \alpha_y\ \psi_y\ \beta_{xu}^1\ \beta_{xu}^2 \ldots \beta_{xu}^{nu-1}\ \beta_{xl}^1\ \beta_{xl}^2 \ldots \beta_{xl}^{nl-1}\ \beta_{yu}^1\ \beta_{yu}^2 \ldots \beta_{yu}^{nu-1}\ \beta_{yl}^1\ \beta_{yl}^2 \ldots \beta_{yl}^{nl-1}\ (\partial w_u/\partial x)\ (\partial w_u/\partial y)\ (\partial w_l/\partial x)\ (\partial w_l/\partial y)\}^T$$

$\{\beta\} = \{u_o\ v_o\ \theta_x\ \theta_y\ u_u\ v_u\ u_l\ v_l\}^T$ whereas elements of [C] will depend on material properties.

The lacuna of C_1 continuity can be mitigated by defining the derivatives of transverse displacement at both facesheet (upper and lower) in terms of displacements u_o, v_o, w_o, θ_x, θ_y, u_u, v_u, u_l, v_l. The last two elements of vector {A} assists in defining the derivatives of transverse displacement. On employing above equations, eq. (2) and eq. (3) can be written as

$$\begin{aligned} U &= b_1 u_0 + b_2 v_0 + b_3\theta_x + b_4\theta_y \\ &\quad + b_5 u_u + b_6 v_u + b_7 u_l + b_8 v_l \end{aligned} \quad (11)$$

$$\begin{aligned} V &= c_1 u_0 + c_2 v_0 + c_3\theta_x + c_4\theta_y \\ &\quad + c_5 u_u + c_6 v_u + c_7 u_l + c_8 v_l \end{aligned} \quad (12)$$

Here the $b_i S$ and $c_i S$ (coefficient of U and V) are function of material properties, thickness coordinates and unit step function. Now the generalized displacement vector {S} can be expressed with the assistance of Eqs. (4), (5), (6), (11), (12) as:

$$\{S\} = \{u_o\ v_o\ w_o\ \theta_x\ \theta_y\ u_u\ v_u\ w_u\ u_l\ v_l\ w_l\}^T$$

If N_i is the shape function at node i, n_n, is the number of nodes per element and S_i is the Displacement vector at node i, then generalized displacement vector $\{S(\varpi)\}$ can be written as

$$\{S(\varpi)\} = \sum_{i=1}^{n_n} N_i(\varpi) S_i(\varpi) \quad (13)$$

If Cartesian strain-displacement matrix is represented by $[A]$ then strain vector can be written as

$$\{\varepsilon(\varpi)\} = [A(\varpi)]\{S(\varpi)\} \quad (14)$$

If U_s = strain energy, U_{ext} = external in-plane load energy, $[A(\varpi)]$ = Random strain displacement matrix then the elemental potential energy (PE) is expressed as

$$\begin{aligned} PE = U_s - U_{ext} &= \frac{1}{2}\iint \{S\}^T [A(\varpi)]^T [E(\varpi)][A(\varpi)]\{S\}dxdy \\ &\quad -\frac{1}{2}\iint \{S\}^T [A(\varpi)]^T [G(\varpi)][A(\varpi)]\{S\}dxdy \quad () \\ &= \frac{1}{2}\{S\}^T[K_e(\varpi)]\{S\} - \frac{1}{2}\lambda\{S\}^T[K_G(\varpi)]\{S\} \end{aligned}$$

where,

$$[E] = \sum_{k=1}^{n}\int [H]^T[Q_k][H]\,dz,$$

$$[G] = \sum_{k=1}^{n}\int [H]^T[S^i][H]\,dz,$$

stress matrix $[S^i]$ can be written as

$$[S^i] = \begin{bmatrix} \sigma_{xx} & \tau_{xy} & 0 & 0 & 0 & 0 \\ \tau_{xy} & \sigma_{yy} & 0 & 0 & 0 & 0 \\ 0 & 0 & \sigma_{xx} & \tau_{xy} & 0 & 0 \\ 0 & 0 & \tau_{xy} & \sigma_{yy} & 0 & 0 \\ 0 & 0 & 0 & 0 & \sigma_{xx} & \tau_{xy} \\ 0 & 0 & 0 & 0 & \tau_{xy} & \sigma_{yy} \end{bmatrix}$$

and strain displacement matrix $[A] = [A_1\ A_2 \ldots]$

$$[A_i] = \begin{bmatrix} \dfrac{\partial N_i}{\partial x} & 0 \\ 0 & \dfrac{\partial N_i}{\partial y} \\ \dfrac{\partial N_i}{\partial y} & \dfrac{\partial N_i}{\partial x} \end{bmatrix}$$

Stochastic elastic stiffness matrix $[K_e(\varpi)] = \int [A(\varpi)]^T\,[E(\varpi)][A(\varpi)]dx$ and geometric stiffness matrix $[K_G(\varpi)] = \int [A(\varpi)]^T\,[G(\varpi)][A(\varpi)]dx.$ If stochastic buckling load factor is denoted by $\lambda(\varpi)$ then the PE equilibrium equation is minimized with respect to {S} and can be written as

$$[K_e(\varpi)]\{S\} = \lambda(\varpi)[K_G(\varpi)]\{S\} \quad (16)$$

The stiffness matrix of global response is stored in a single array using skyline technique and simultaneous iteration technique is used to solve the stochastic buckling equations.

3. Radial basis function based surrogate modelling

Radial basis function comprises of input layer, output layer and a layer of RBF neurons in between them. The number of nodes in output layer is equal to the types (category) of data filtered from a layer of RBF neurons. Each RBF neurons stores a prototype and a new input variable is categorized on the basis of Euclidean distance between input and prototype (computed by each neuron). Architecture of RBF network (McCormick C. (2013)) is illustrated in figure 4. The Euclidean distances of linear combination presented in surrogate based model is represented as (Dey *et al*. (2017))

$$\hat{Y}(x) = \sum_{p=1}^{M} w_p \phi_p(X, x_p) \tag{17}$$

Weight determined by using the least-squares method is represented by w_p, number of sampling points by M while p-th basis function determined at the sampling point x_p is described by $\phi_p(X, x_p)$.

RBF model is represented by using radial function, which is expressed as,

$$F(x) = \frac{1}{\sqrt{1 + \frac{(x-c)^T\ (x-c)}{r^2}}} \tag{18}$$

(For inverse multi-quadratic)

$$F(x) = \exp\left(-\frac{(x-c)^T\ (x-c)}{r^2}\right) \tag{19}$$

(For Gaussian)

$$F(x) = \frac{1}{1 + \frac{(x-c)^T\ (x-c)}{r^2}} \tag{20}$$

(For Cauchy)

$$F(x) = \sqrt{1 + \frac{(x-c)^T\ (x-c)}{r^2}} \tag{21}$$

(For multi-quadratic)

Here $r^2 = 1$ is assumed to be fixed for the application of Gaussian basis function. Since the function value from approximate function equals to that of true function, it exactly passes through all the sampling point. It acts in a similar way to that of brain. It is having versatile problem solving ability like pattern recognition, prediction, optimization, associative memory and control tool which is modelled as per our biological brain, which made it of keen interest to researcher.

4. RBF based stochastic buckling analysis

The effect of core thickness, facesheet material properties, ply orientation angle and number of laminate on the global buckling load response of sandwich panel in the stochastic regime is investigated by simultaneously varying all input parameters. Effect of degree of stochasticity in material properties, ply orientation angle, and thickness are also analyzed individually. Layer wise (bottom-up) random variable approach is employed to investigate the stochastic buckling behavior of sandwich panel.

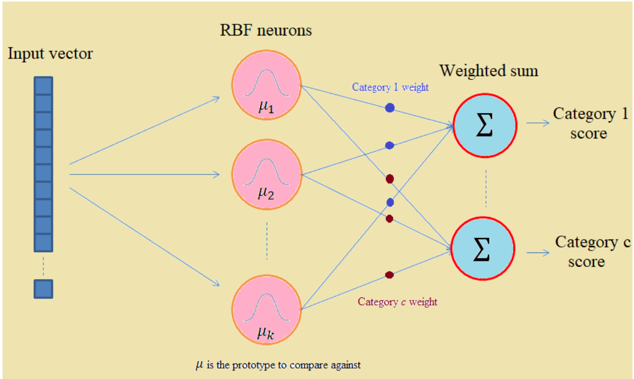

Fig. 4 Architecture of radial basis function network

(a) Effect of ply orientation angle, considering combined stochasticity

$$\Theta(\theta) = \Xi[\theta(\varpi), t(\varpi), P(\varpi)]\ ;$$

$$t(\varpi) = t_c(\varpi) + t_f(\varpi), P(\varpi) = P_c(\varpi) + P_f(\varpi)$$

(b) Effect of core thickness, considering combined stochasticity

$$\Theta(t_c) = \Xi[\theta(\varpi), t(\varpi), P(\varpi)]$$

(c) Effect of number of laminate, considering combined stochasticity

$$\Theta(n) = \Xi[\theta(\varpi), t(\varpi), P(\varpi)]$$

(d) Effect of facesheet material properties, considering combined stochasticity

$$\Theta(P_f) = \Xi[\theta(\varpi), t(\varpi), P(\varpi)]$$

(e) Effect of ply orientation angle, considering individual stochasticity

$$\Theta(\theta) = \Xi[\theta(\varpi),\ t,\ P]$$

(f) Effect of degree of stochasticity in core thickness, considering individual variation

$$\Theta(\Delta t_c(\varpi)) = \Xi[\theta,\ t(\varpi),\ P]$$

(g) Effect of degree of stochasticity in facesheet thickness, considering individual variation

$$\Theta(\Delta t_f(\varpi)) = \Xi[\theta,\ t(\varpi),\ P]$$

(h) Effect of degree of stochasticity in facesheet material properties, considering individual variation

$$\Theta(\Delta P_f(\varpi)) = \Xi[\theta,\ t,\ P(\varpi)]$$

(i) Effect of degree of stochasticity in core material properties, considering individual variation

$$\Theta(\Delta P_c(\varpi)) = \Xi[\theta,\ t,\ P(\varpi)]$$

In general, the accepted zone of tolerance during a manufacturing process for variabilities in material or geometric properties is standardized by the manufacturers. In this study, the representative degree of stochasticity with respect to mean deterministic value is considered as ±10°

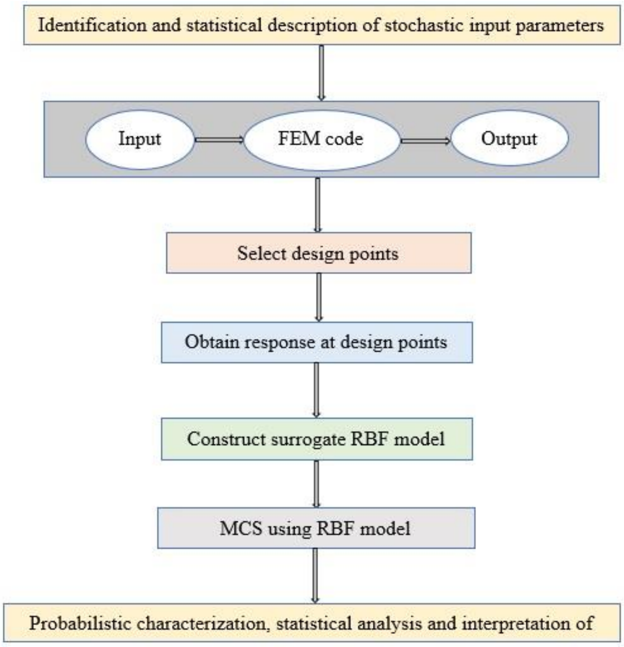

Fig. 5 Flow chart of RBF based probabilistic analysis

for ply-orientation angle (θ), whereas ±10% for face sheet material properties (P_f), face sheet thickness (t_f), core material properties (P_c) and core thickness (t_c). Moreover, the prescribed level of percentage of stochasticity is benchmarked as per the typical industry standards of various aircraft manufacturers. In a complex problem like uncertainty analysis of sandwich panels, three aspects are needed to tackle. The first one is the modelling of source-uncertainty for probabilistic analysis. The second aspect is the uncertainty propagation from elemental input level to the overall output response quantification. The last concern is to follow the bottom-up framework. In the present analysis surrogate based uncertainty propagation technique is observed due to being a conventional Monte Carlo simulation method as the computationally intensive approach. The computational efficiency for buckling analysis of sandwich panel is achieved by employing a RBF based surrogate modelling framework in conjunction with the finite element model as illustrated in figure 5.

5. Results and Discussion

In present study, buckling load of laminated sandwich panel (8 laminate on both facesheet) having thickness (t) = 1cm, length (l) = 10cm, and width (b) = 10cm is calculated in stochastic regime for four different boundary conditions (SSSS, CFCF, CCCC, and SCSC; F-Free, S-Simply supported, C-Clamped). Numerical results for sandwich panel having t_c = 0.8 cm, t_f = 0.2 cm, and θ = (90°/0°/90°/0°/90°/0°/90°/0°) are presented based on the material properties (Kollar (2003)) given in the literature

(a) For core:

$E_1=E_2=E_3=0.5$GPa, $G_{12}=G_{13}=0.4$GPa, $G_{23}=0.2$GPa, $\upsilon_{12}=\upsilon_{13}=\upsilon_{23}=\upsilon_{32}=0.27$, $\upsilon_{21}=\upsilon_{31}=0.006$, ρ =1000 kg/m^3 and

(b) For facesheet (P_1):

$E_1=38.6$GPa, $G_{12}=G_{13}=4.14$GPa, $E_2=E_3=8.27$GPa, $G_{23}=1.656$GP, $\upsilon_{12}=\upsilon_{13}=\upsilon_{23}=\upsilon_{32}=0.26$, $\upsilon_{21}=\upsilon_{31}=0.006$ ρ =2600 kg/m^3

(c) For facesheet (P_2):

$E_1=43$GPa, $G_{12}=G_{13}=4.5$GPa, $E_2=E_3=8.9$GPa, $G_{23}=1.8$GPa, $\upsilon_{12}=\upsilon_{13}=\upsilon_{23}=\upsilon_{32}=0.27$, $\upsilon_{21}=\upsilon_{31}=0.006$, ρ=2490 kg/m^3

5.1 Validation and convergence study

In the case of surrogate-based probabilistic analysis, two types of validation are needed to carry out. First one is finite element validation of code, and another one is the surrogate model (RBF) validation to check its accuracy and predictability. For FE validation of the code, convergence study is carried out for deterministic buckling load as presented in Table 1 along with the previous result of reddy (1984), Kant and Manjunath (1998). The result shows good agreement of present work with previous works. HOZT is applied in present FE formulation, which is different from the literature used for deterministic validation. The numerical value of the buckling load decreases with an increase in mesh size from 8x8 to 12x12, and their difference is negligible (~ 0.001%). It demonstrates the convergence of present finite element formulation for a mesh size of is 8x8. The difference in converged mesh size result and the published literature result also lies within the acceptable limit (~0.05 to 0.99%). The accuracy of the RBF based surrogate model is estimated by three different means:

(a) Convergence study and absolute percentage error analysis

(b) Probability density function (PDF) plot

(c) Scatter plot of RBF surrogate model with original finite element (FE) model

The convergence study (refer to Table 2) for maximum, minimum, mean and standard deviation (SD) value of stochastic buckling load obtained through constructed RBF surrogate model of different sample sizes (M=64, 128, 256, and 512) show that, as the number of sample size for surrogate model formation increases result obtained through it reaches closer to that of full scale direct MCS result. It is further quantified in terms of absolute percentage error (refer to figure 6) for getting the optimum number of sample size required for surrogate model formation. This is calculated as

$$\left[\left|\frac{Direct\ MCS\ \ data - RBF\ based\ MCS\ data}{Direct\ MCS\ \ data}\right| \times 100\%\right]$$

It shows below 0.2% mean absolute percentage error for 256 number of sample size. Hence it is further examined up to 256 number of sample size. PDF of CCCC sandwich panel are portrayed for the result obtained from Direct Monte Carlo simulation and RBF approach having 64, 128 and 256 sample run. PDF plot presented in Figure 7(a) indicates insignificant discrepancy of RBF model in

Table 1 Non-dimensional deterministic buckling load for simply supported laminated composite [0°/90°/0°] plate ($E_{11}/E_{22} = 40$)

Span thickness ratio	Present FEM 4×4	Present FEM 8×8	Present FEM 12×12	Reddy (1984)	Kant and Manjunath (1998)
10	21.9064	21.8991	21.8988	22.1207	22.0671
50	35.2596	35.2083	35.2069	35.2293	35.2248
100	36.0361	35.9185	35.9168	35.9211	35.9211

Table 2 Convergence study of result obtained by using RBF surrogate model constructed through different sample size in comparison to full scale direct MCS approach

Stochastic buckling load value	MCS(10000)	Sample size 64	128	256	512
Max	1.9964e+08	1.9108e+08	1.9041e+08	1.9326e+08	1.9494e+08
Min	1.4033e+08	1.5008e+08	1.4561e+08	1.4203e+08	1.4122e+08
Mean	1.6831e+08	1.7016e+08	1.6867e+08	1.6816e+08	1.6826e+08
SD	9.3958e+06	5.5946e+06	6.8443e+06	8.1775e+06	8.6464e+06

comparison to the original finite element based MCS model, establishes the reliability of RBF based FE approach. For further validation of the RBF model as the surrogate of the actual finite element model scatter plots (Figure 7(b-d)) are used. A negligible discrepancy of points from the diagonal line in scatter plot indicates the high prediction capability and applicability of RBF model instead of time-consuming conventional finite element model for a set of random input parameters (sixty (60) number of random input parameters in case of combined variation). On considering both PDF and scatter plot, 256 sample size is used for further analysis to save computational time and cost without compromising with accuracy.

5.2 Numerical results for stochastic buckling analysis

The RBF based FE model is validated in the previous section. Now, the numerical results for probabilistic critical buckling load are presented in this section. The critical buckling load corresponding to least Eigen value is considered as useful in most of the engineering applications. It is to be noted that the proposed RBF based FE approach requires only 256 number of original FE based direct MCS iteration although the same numbers of samples as in direct MCS (10,000 samples) are used to characterize the probability density of buckling load. Therefore, remarkable computational time and effort reduced compared to direct MCS approach. This method provides an affordable way to calculate stochastic buckling load accurately and precisely in very less time.

Effect of ply-orientation angle on global response of structure corresponding to different boundary condition is presented in figure 8. It is observed that response bound is maximum for CCCC boundary condition followed by SCSC, SSSS and minimum for CFCF as illustrated in figure 8.

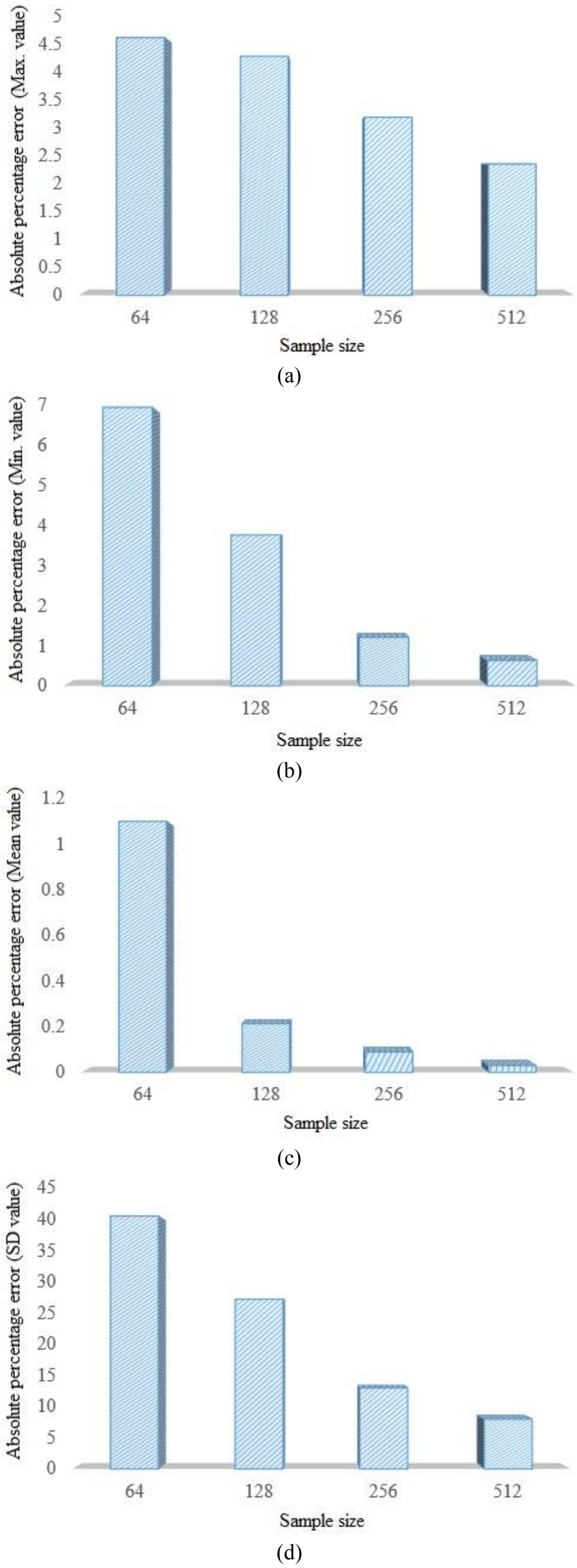

Fig. 6 Absolute percentage error for (a) Max. value (b) Min. value (c) Mean value and (d) Standard deviation value of buckling load for surrogate RBF model formation considering combined variation and CCCC boundary condition

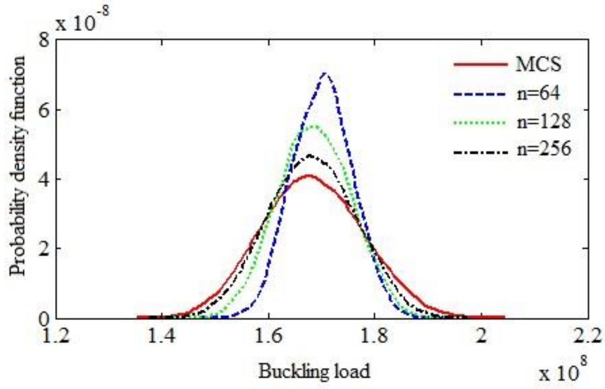

(a)

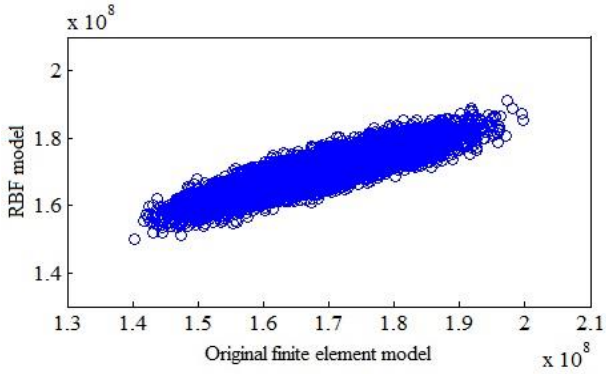

(b)

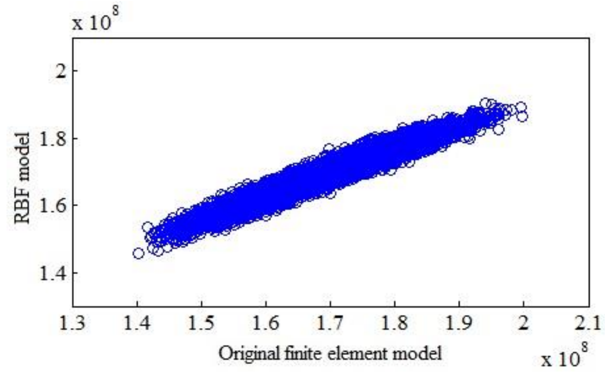

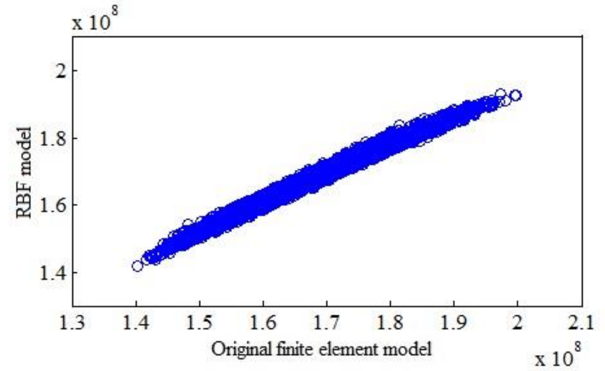

Fig. 7 (a) Probability density function plot for different sample size (*M*=64,128,256) with respect to MCS; Scatter plot for RBF model of (b) 64 sample size, (c) 128 sample size, (d) 256 sample size with original FE model considering combined variation and CCCC boundary condition

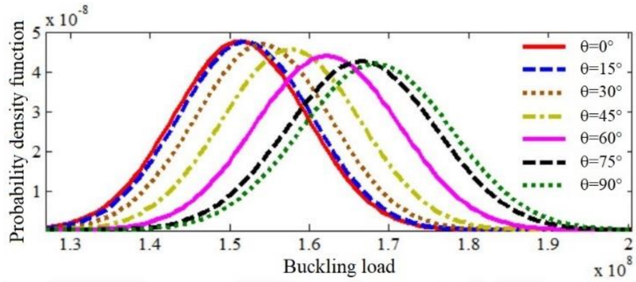

(a)

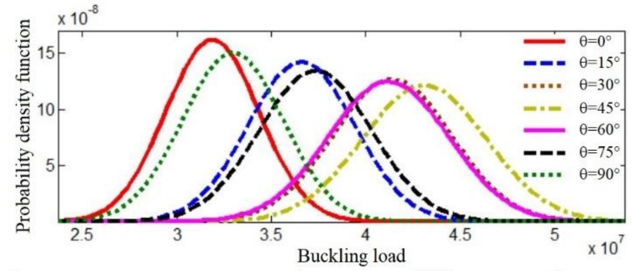

(b)

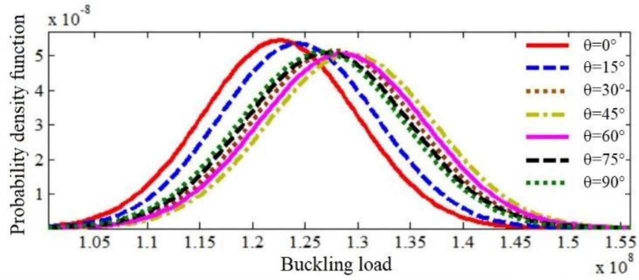

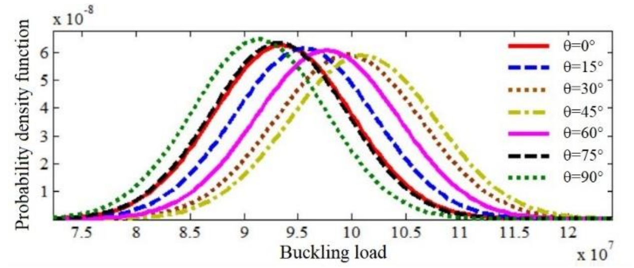

Fig. 8 Stochastic buckling response of composite sandwich panel having different ply orientation angle considering combined variation for (a) CCCC (b) CFCF (c) SCSC (d) SSSS boundary condition.

Mean value is observed to be increasing with increase in ply-orientation angle with maximum at 90° and minimum at 0° in case of CCCC sandwich panel. It is observed to be maximum at 45° and minimum at 0° ply-orientation angle in case of SCSC and CFCF whereas it is maximum at 45° and minimum at 90° ply angle in case of SSSS sandwich panel. Effect of core thickness on global buckling response of sandwich panel for combined variation of all input parameter is shown in figure 9. A common trend is observed for all B.C that the mean buckling load decreases with an increase in core thickness. Effect of the different number of facesheet layer having the same core and facesheet thickness, considering variation in all random input parameter is depicted in figure 10. It shows that, with an increase in the number of layer buckling load decreases but

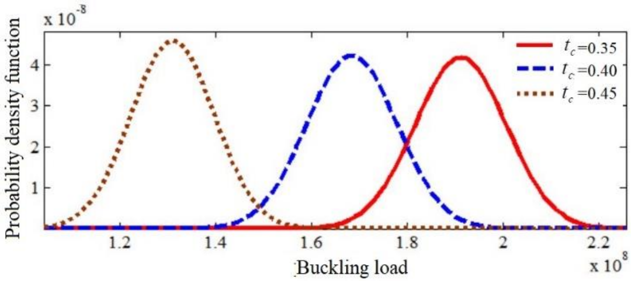

(a)

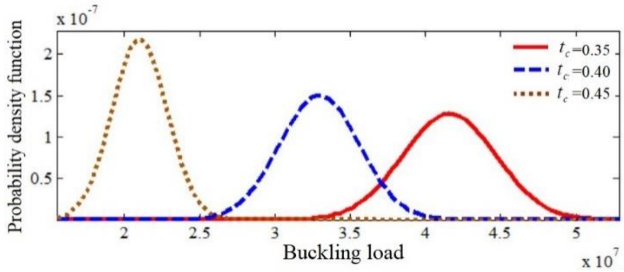

(b)

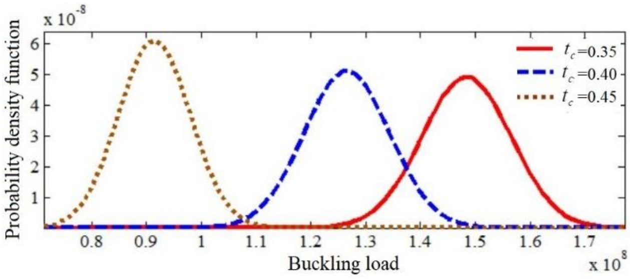

(c)

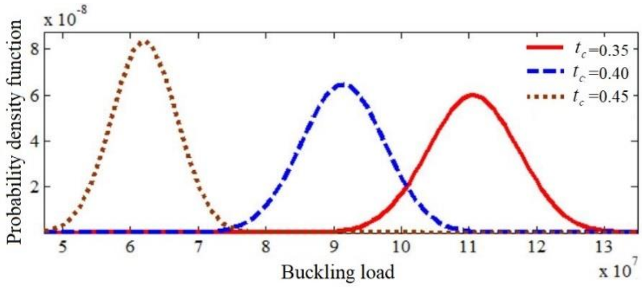

(d)

Fig. 9 Stochastic buckling response of sandwich panel having different core thickness considering combined variation for (a) CCCC (b) CFCF (c) SCSC (d) SSSS boundary condition

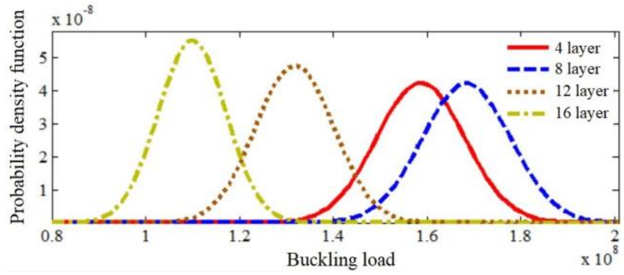

(a)

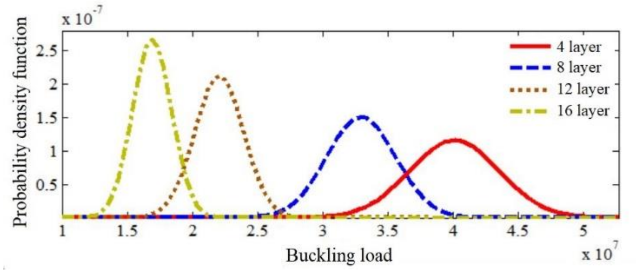

(b)

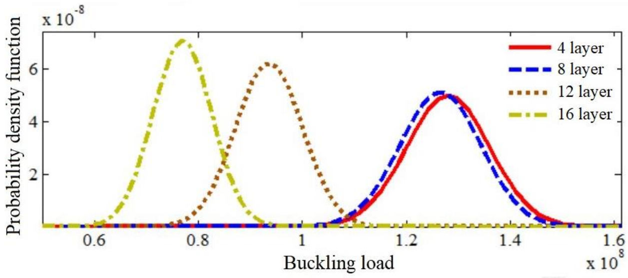

(c)

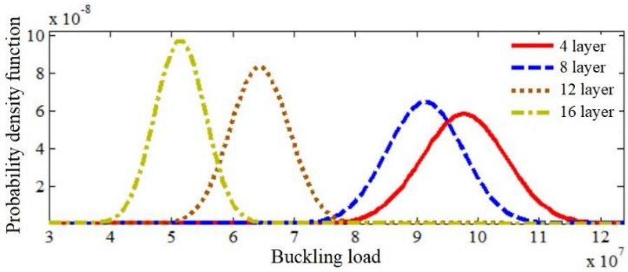

(d)

Fig. 10 Stochastic buckling response of sandwich panel having different number of facesheet layer considering combined variation for (a) CCCC (b) CFCF (c) SCSC (d) SSSS boundary condition

CCCC shows exceptional behavior having least buckling load for 8-layer facesheet. Figure 11 represents the effect of facesheet material properties, considering the combined variation of all the parameters. It is noted that the buckling load of P_1 is less than that of P_2 irrespective of the end condition. Now the effect of individual variation of input parameters with different degree of stochasticity is investigated to know the effect of a particular uncertain parameter on the global response of the structure. The effect of different ply orientation angle considering Stochasticity in only ply-angle is depicted in figure 12. It illustrates the same maximum and minimum trend to that in combined Variation (refer figure 8), but their probability density is varying in a different fashion. Effect of different degree of stochasticity in core thickness is illustrated in figure 13 which shows that the sparsity increases with increase in fluctuations (i.e., the degree of stochasticity). Variation in buckling load with different degree of stochasticity in facesheet thickness is presented in figure 14. It follows the same trend to that of figure 13. Effect of different degree of stochasticity in only facesheet material properties is depicted in figure 15 whereas the effects of different quantity of uncertainty in core material properties are shown in figure 16. A common behavior is noticed that, with an increase in the degree of stochasticity sparsity increases. Figure 17 shows the effect of end condition on buckling behavior of 8 layered sandwich panel having 0/90

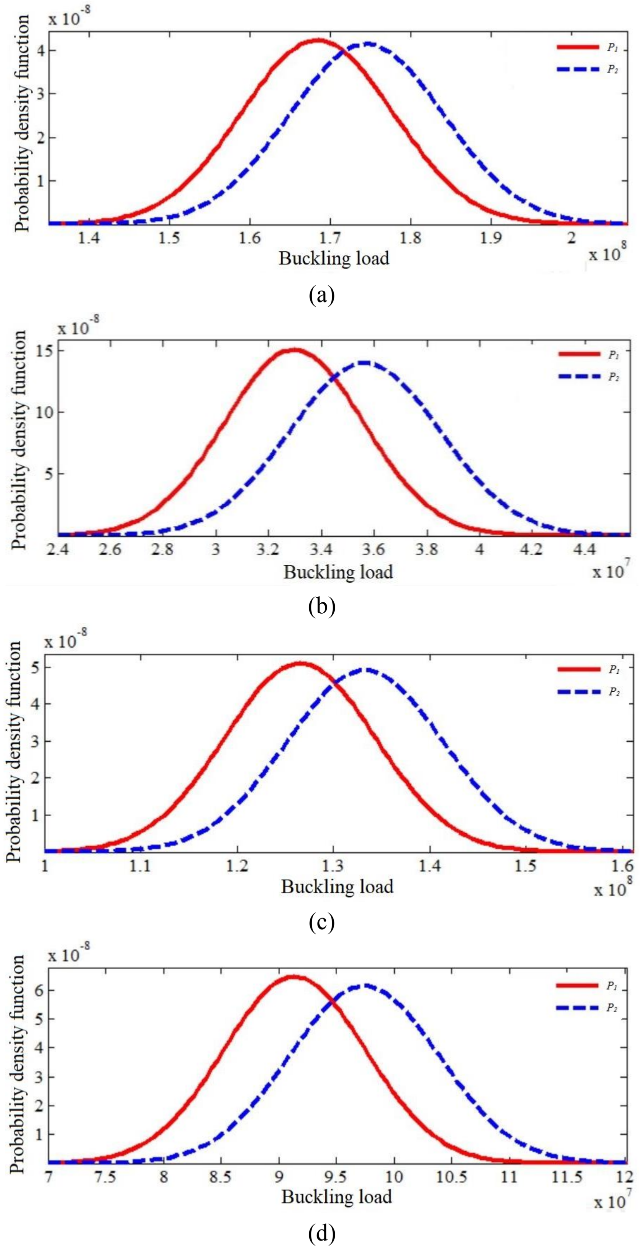

Fig. 11 Stochastic buckling response of sandwich panel having different material properties considering combined variation for (a) CCCC (b) CFCF (c) SCSC (d) SSSS boundary condition

ply orientation angle considering combined stochasticity in material as well as geometric properties. It is observed that there is a significant change in the value of buckling load with boundary condition (B.C.). The increasing amount of buckling load follows the order of CFCF, SSSS, SCSC, and CCCC, respectively. Hence, the maximum amount of buckling load is observed in CCCC whereas minimum in case of CFCF end condition. Sensitivity analysis suggests that which parameter is more affecting the global buckling response of the system. Sensitivity analysis is performed by considering the individual effect of all the parameters for all four boundary conditions.

As per sensitivity analysis (refer figure 18) performed in present study effect of panel thickness followed by material

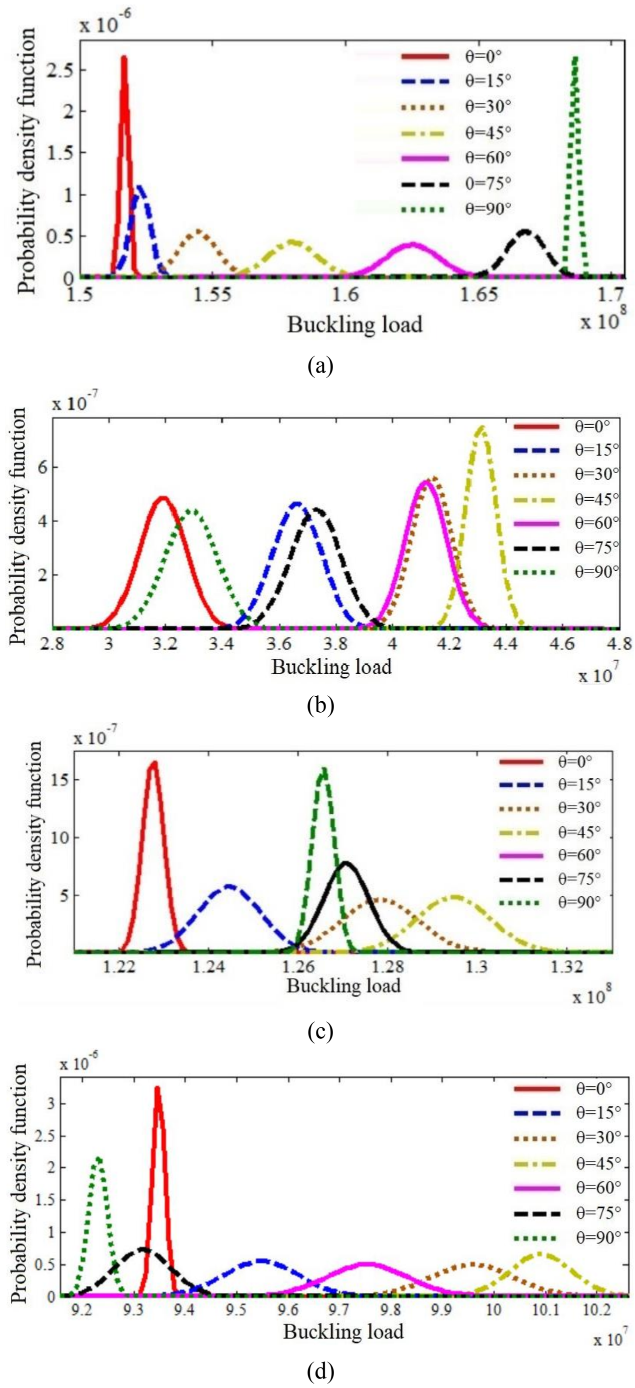

Fig. 12 Stochastic buckling response of sandwich panel having different ply-orientation angle considering individual variation $\theta(\varpi)$ for (a) CCCC (b) CFCF (c) SCSC (d) SSSS boundary condition

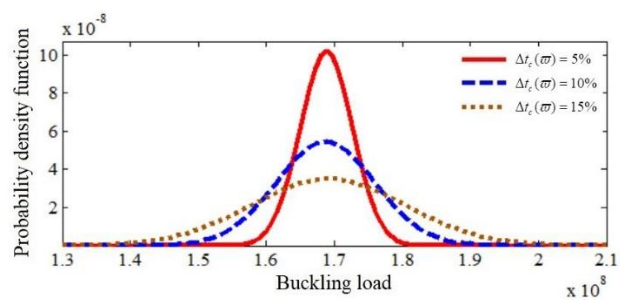

(a)

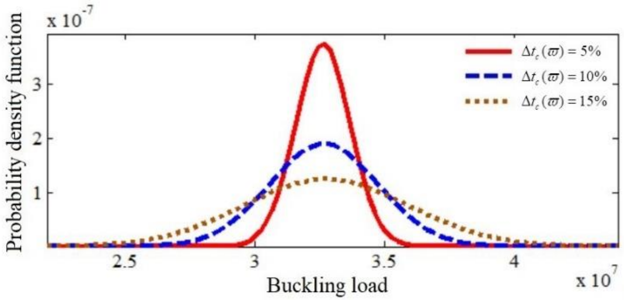

(b)

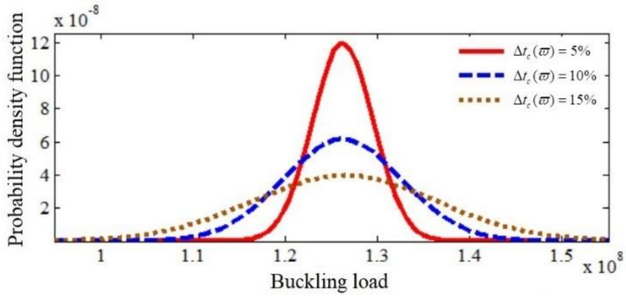

(c)

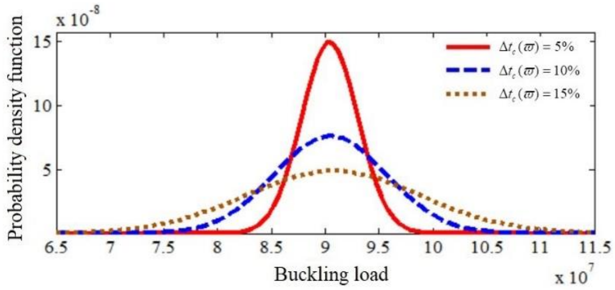

(d)

Fig. 13 Stochastic buckling response of sandwich panel considering different degree of stochasticity in core thickness $t_c(\varpi)$ for (a) CCCC (b) CFCF (c) SCSC (d) SSSS boundary condition

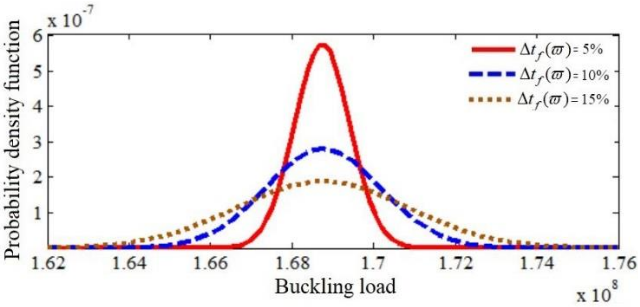

(a)

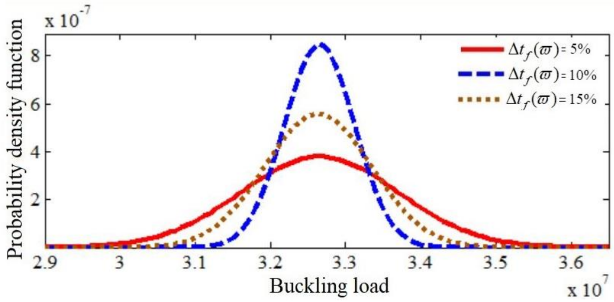

(b)

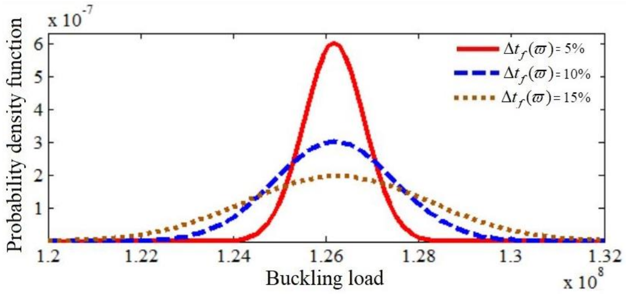

(c)

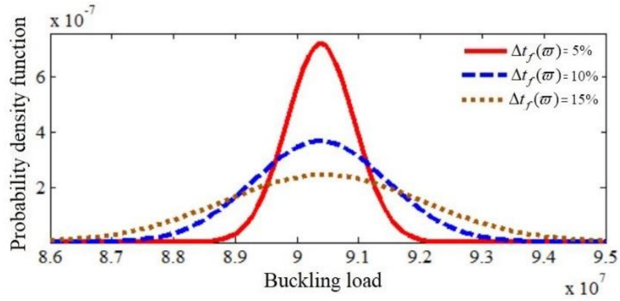

(d)

Fig. 14 Stochastic buckling response of sandwich panel considering different degree of stochasticity in facesheet thickness $t_f(\varpi)$ only for (a) CCCC (b) CFCF (c) SCSC (d) SSSS boundary condition

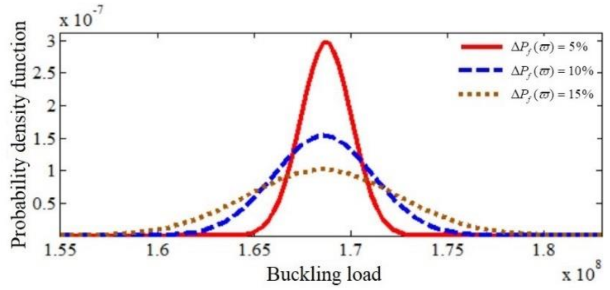

(a)

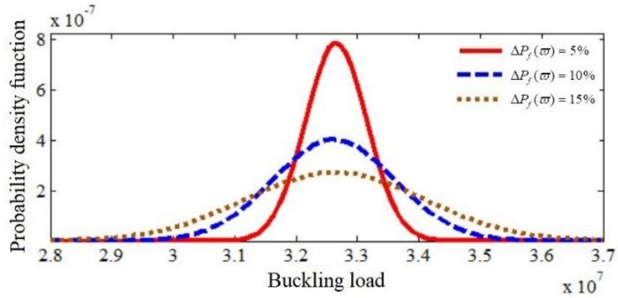

(b)

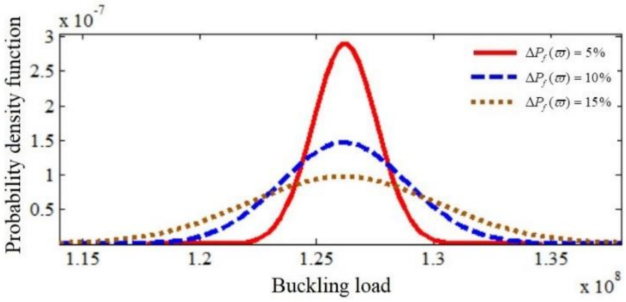

(c)

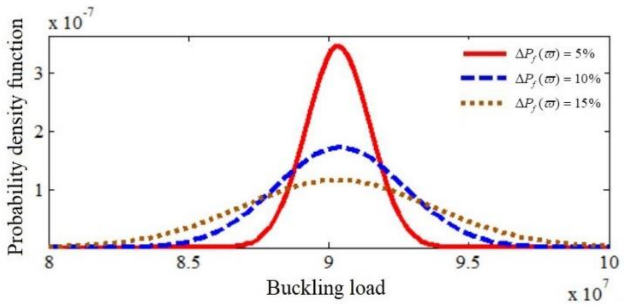

(d)

Fig. 15 Stochastic buckling response of sandwich panel considering different degree of stochasticity in facesheet material properties $P_f(\varpi)$ only for (a) CCCC (b) CFCF (c) SCSC (d) SSSS boundary condition

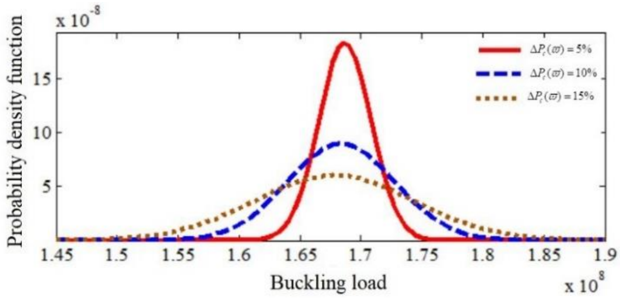

(a)

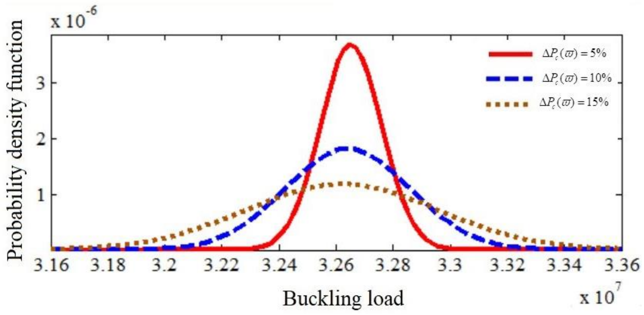

(b)

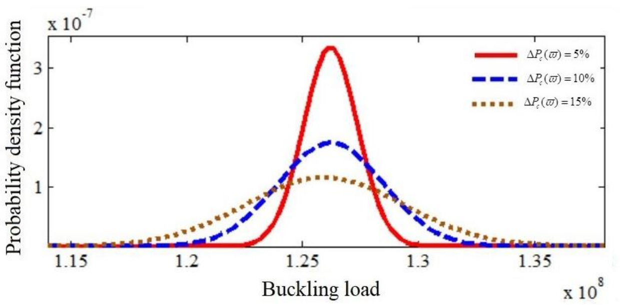

(c)

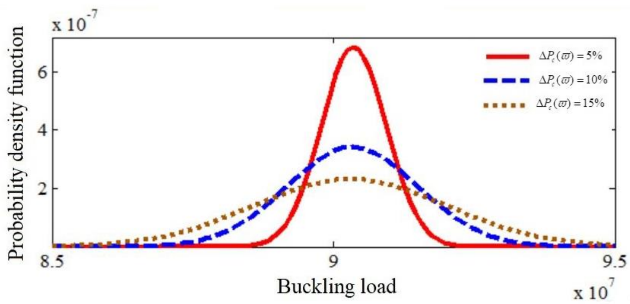

(d)

Fig. 16 Stochastic buckling response of sandwich panel considering different degree of stochasticity in core material properties $P_c(\varpi)$ only for (a) CCCC (b) CFCF (c) SCSC (d) SSSS boundary condition

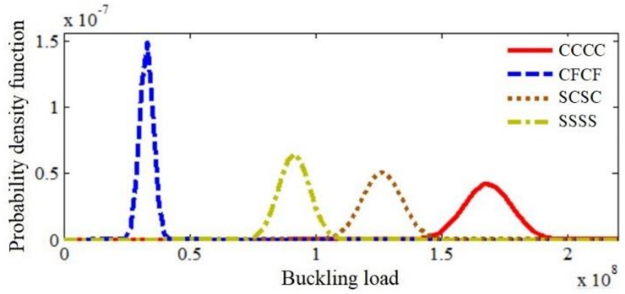

Fig. 17 Stochastic response of CCCC, CFCF, SCSC, SSSS boundary conditioned Sandwich panel considering combined stochasticity in all properties.

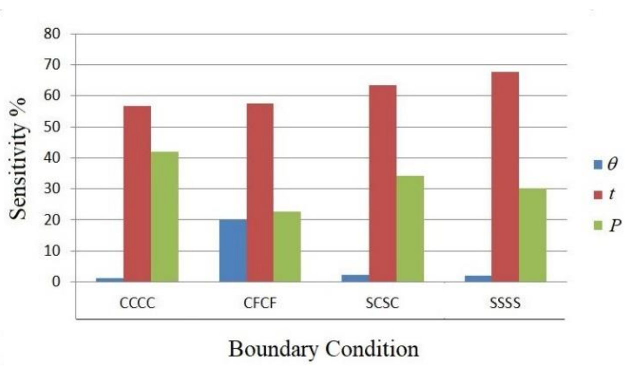

Fig. 18 Sensitivity of ply orientation angle (θ) thickness (t) and material properties (P) for (a) CCCC (b) CFCF (c) SCSC (d) SSSS boundary conditions

properties (both core and face sheet) is highly significant on buckling load of the panel, whereas ply-orientation angle has an insignificant effect on it.

6. Conclusions

The present study includes a generalized algorithm for stochastic buckling load of sandwich panels by employing an efficient RBF based finite element simulation approach. This paper presents a radial basis function based bottom-up stochasticity propagation approach for critical buckling load calculation of sandwich panel (consisting of laminated composite facesheet and soft core) in a probabilistic regime. It is noticed that RBF gives a significantly higher level of computational efficiency with respect to direct Monte Carlo simulation without compromising with the accuracy. The novelty in the present study lies in uncertainty quantification of buckling load of a sandwich panel for several decisive elements such as ply-orientation angle, thickness, material properties and boundary conditions due to stochasticity in system properties. Based on radial basis function coupled with finite element approach, it demonstrates a significant level of savings in terms of computation time and cost. In case of stochastic buckling analysis, the computational efficiency is reported to achieve by more than 1/39 times to that of conventional Monte Carlo simulation technique on employing radial basis function based surrogate model in conjunction with finite element model. The individual and combined stochastic variations in random input parameters are used to depict the probability distribution plot for buckling behavior of sandwich panel. A sensitivity analysis is conducted to scrutinize the comparative significance of different parameters in the global response of the structure. The result of such analysis could be quite crucial in the design of a composite sandwich structure. The thickness of the panel is found to be most sensitive followed by material properties and ply-orientation angle. The probabilistic result presented in this paper illustrates that the buckling behavior of soft core sandwich panel is remarkably deviating from their deterministic value due to inexorable uncertainty source present in real life problem. Hence it is necessary to consider the effect of stochasticity in the design parameter for better reliability and sustainability. The proposed surrogate based finite element approach for uncertainty propagation can be further extended for higher order buckling response of the complex structure.

Acknowledgement

The first author would like to acknowledge the financial support received from MHRD, Govt. of India during the period of this research work.

References

Al-Shamary, A.K., Karakuzu. R. and Özdemir, O. (2016), “Low-velocity impact response of sandwich composites with different foam core configurations”, *J. Sandwich Struct. Mater.*, **18**(6), 754-768. https://doi.org/10.1177/1099636216653267.

Alamatian, J. and Hosseini-Nejad, G.M. (2017), “An efficient explicit framework for determining the lowest structural buckling load using Dynamic Relaxation method”, *Mech. Based Design Struct. Machines*, **45**(4), 451-462. https://doi.org/10.1080/15397734.2016.1238765.

Bart-Smith, H., Hutchinson, J.W. and Evans, A.G. (2001), “Measurement and analysis of the structural performance of cellular metal sandwich construction”, *J. Mech. Sci.*, **43**(8), 1945-1963. https://doi.org/10.1016/S0020-7403(00)00070-9.

Caliskan, U. and Apalak, M.K. (2017), “Low velocity bending impact behavior of foam core sandwich beams: Experimental”, *Compos. Part B Eng.*, **112**, 158-175. https://doi.org/10.1016/j.compositesb.2016.12.038.

Chalak, H.D., Chakrabarti, A. and Sheikh A.H. (2015), “Iqbal MA. Stability analysis of laminated soft core sandwich plates using higher order zig-zag plate theory”, *Mech. Adv. Mater. Struct.*, **22**(11), 897-907. https://doi.org/10.1080/15376494.2013.874061.

Deshpande, V.S. and Fleck, N.A. (2001), “Collapse of truss core sandwich beams in 3-point bending”, *J. Solid. Struct.*, **38**(36-37),6275-305. https://doi.org/10.1016/S0020-7683(01)00103-2.

Deshpande, V.S. and Fleck, N.A. (2003) “Energy absorption of an egg-box material”, *J. Mech. Phys. Solid.*, **51**(1), 187-208. https://doi.org/10.1016/S0022-5096(02)00052-2.

Dey, S., Mukhopadhyay, T. and Adhikari, S. (2017), “Metamodel based high-fidelity stochastic analysis of composite laminates: A concise review with critical comparative assessment”, *Compos. Struct.*, **171**, 227-250. https://doi.org/10.1016/j.compstruct.2017.01.061.

El-Haina, F., Bakora, A., Bousahla, A.A., Tounsi, A. and Mahmoud, S.R. (2017), “A simple analytical approach for thermal buckling of thick functionally graded sandwich plates”, *Struct. Eng. Mech.*, **63**(5), 585-595. http://dx.doi.org/10.12989/sem.2017.63.5.585.

Elmossouess, B., Kebdani, S., Bouiadjra, M.B. and Tounsi, A. (2017), “A novel and simple HSDT for thermal buckling response of functionally graded sandwich plates”, *Struct. Eng. Mech.*, **62**(4), 401-415. http://dx.doi.org/10.12989/sem.2017.62.4.401.

Fan, H., Zhou, Q., Yang, W. and Jin gjing, Z. (2010), “An experiment study on the failure mechanisms of woven textile sandwich panels under quasi-static loading”, *Compos. Part B Eng.*, **41**(8), 686-92. https://doi.org/10.1016/j.compositesb.2010.07.004.

Golchi, M., Talebitooti, M. and Talebitooti, R. (2018), “Thermal buckling and free vibration of FG truncated conical shells with stringer and ring stiffeners using differential quadrature method”, *Mech. Based Design Struct. Machines*, 1-28. https://doi.org/10.1080/15397734.2018.1545588.

Gupta, A. and Talha, M. (2018), “Influence of initial geometric imperfections and porosity on the stability of functionally graded material plates”, *Mech. Based Design Struct. Machines*, 1-9. https://doi.org/10.1080/15397734.2018.1449656.

Hohe, J. (2015), “Load and frequency interaction effects in dynamic buckling of soft core sandwich structures”, *Compos. Struct.*, **132**, 1006-1018. https://doi.org/10.1016/j.compstruct.2015.07.011.

Ikeda, K., Ohsaki, M., Sudo, K. and Kitada, T. (2009), “Probabilistic analysis of buckling loads of structures via extended Koiter law”, *Struct. Eng. Mech.*, **32**(1), 167-178.

Kacar, I. and Yildirim, V. (2016), “Free vibration/buckling analyses of noncylindrical initially compressed helical composite springs”, *Mech. Based Design Struct. Machines*, **44**(4), 340-353. https://doi.org/10.1080/15397734.2015.1066687.

Kahya, V. (2016), “Buckling analysis of laminated composite and sandwich beams by the finite element method”, *Compos. Part B Eng.*, **91**, 126-134. https://doi.org/10.1016/j.compositesb.2016.01.031.

Kant, T. and Manjunath, B.S. (1998), “An unsymmetric FRC laminated finite element model with 12 degree of freedom per node”, *Eng Comput.*, **5**(4), 300-308.

Karsh, P.K., Mukhopadhyay, T. and Dey, S. (2018a), “Spatial vulnerability analysis for the first ply failure strength of composite laminates including effect of delamination”, *Compos. Struct.*, **184**, 554-567. https://doi.org/10.1016/j.compstruct.2017.09.078.

Karsh, P.K., Mukhopadhyay, T. and Dey, S. (2018b), “Stochastic dynamic analysis of twisted functionally graded plates”, *Compos. Part B Eng.*, **147**, 259-278. https://doi.org/10.1016/j.compositesb.2018.03.043

Karsh, P.K., Mukhopadhyay, T. and Dey, S. (2018c), “Stochastic Investigation of Natural Frequency for Functionally Graded Plates”, *InIOP Conference Series Mater. Sci. Eng.*, **326**(1), https://doi.org/10.1088/1757-899X/326/1/012003.

Karsh, P.K., Mukhopadhyay, T. and Dey, S. (2019), “Stochastic low-velocity impact on functionally graded plates: Probabilistic and non-probabilistic uncertainty quantification”, *Compos. Part B Eng.*, **159**, 461-480. https://doi.org/10.1016/j.compositesb.2018.09.066.

Khalili, S.M, Kheirikhah, M.M. and Malekzadeh Fard, K. (2015), “Buckling analysis of composite sandwich plates with flexible core using improved high-order theory”, *Mech. Adv. Mater. Struct.*, **22**(4), 233-247. https://doi.org/10.1080/15376494.2012.736051.

Kheirikhah, M.M., Khalili, S.M. and Fard, K.M. (2012), “Biaxial buckling analysis of soft-core composite sandwich plates using improved high-order theory”, *European J. Mech. A/Solids*, **31**(1), 54-66. https://doi.org/10.1016/j.euromechsol.2011.07.003.

Kolahchi, R.A. (2017), “Comparative study on the bending, vibration and buckling of viscoelastic sandwich nano-plates based on different nonlocal theories using DC, HDQ and DQ methods”, *Aerosp. Sci. Technol.*, **66**, 235-248. https://doi.org/10.1016/j.ast.2017.03.016.

Kollar, L.P. and Springer, G.S. (2003), *Mechanics of Compos. Struct.*, Cambridge, United Kingdom.

Kumar, R.R., Mukhopadhyay, T., Pandey, K.M. and Dey, S. (2019), “Stochastic buckling analysis of sandwich plates: The importance of higher order modes”, *J. Mech. Sci.*, **152**, 630-643. https://doi.org/10.1016/j.ijmecsci.2018.12.016.

Lal, A., Kulkarni, N.M. and Singh, B.N. (2015), “Stochastic thermal post buckling response of elastically supported laminated piezoelectric composite plate using micromechanical approach”, *Curv. Layer. Struct.*, **2**(1). https://doi.org/10.1515/cls-2015-0019.

Lal, A., Saidane, N. and Singh, B.N. (2012), “Stochastic hygrothermoelectromechanical loaded post buckling analysis of piezoelectric laminated cylindrical shell panel”, *Smart Struct. Syst.*, **9**(6), 505-534. http://dx.doi.org/10.12989/sss.2012.9.6.505.

Li, J., Tian, X., Han, Z. and Narita, Y. (2016), “Stochastic thermal buckling analysis of laminated plates using perturbation technique”, *Compos. Struct.*, **139**, 1-2. https://doi.org/10.1016/j.compstruct.2015.11.076.

Magnucka-Blandzi, E., Wisniewska-Mleczko, K., Smyczynski, M. J. and Kedzia, P. (2018), “Buckling of a sandwich symmetrical circular plate with varying mechanical properties of the core”, *Appl. Math. Mech.*, **39**(7), 981-992. https://doi.org/10.1007/s10483-018-2347-8.

McCormick, C. (2013), Radial Basis Function Network (RBFN) Tutorial. http://mccormickml.com/2013/08/15/radial-basis-function-network-rbfn-tutorial.

Mohammadimehr, M., Nejad, E.S. and Mehrabi, M. (2018), “Buckling and vibration analyses of MGSGT double-bonded micro composite sandwich SSDT plates reinforced by CNTs and BNNTs with isotropic foam & flexible transversely orthotropic cores”, *Struct. Eng. Mech.*, **65**(4), 491-504. http://dx.doi.org/10.12989/sem.2018.65.4.491.

Moita, J.S., Araújo, A.L., Correia, V.F., Soares, C.M. and Soares, C.M. (2015), “Buckling and geometrically nonlinear analysis of sandwich structures”, *J. Mech. Sci.*, **92**, 154-161. https://doi.org/10.1016/j.ijmecsci.2014.12.008.

Moradi-Dastjerdi, R. and Malek-Mohammadi, H. (2017), “Biaxial buckling analysis of functionally graded nanocomposite sandwich plates reinforced by aggregated carbon nanotube using improved high-order theory”, *J. Sandwich Struct. Mater.*, **19**(6), 736-769. https://doi.org/10.1177/1099636216643425.

Mukhopadhyay, T., Naskar, S., Karsh, P.K., Dey, S. and You, Z. (2018), “Effect of delamination on the stochastic natural frequencies of composite laminates”, *Compos. Part B Eng.*, **154**, 242-256. https://doi.org/10.1016/j.compositesb.2018.07.029.

Muradova, A.D., Kurutz, M. and Stavroulakis, G.E. (2009), “Buckling simulation of a plate embedded in a unilaterally supported environment”, *Mech. Based Design Struct. Machines*, **37**(3), 349-370. https://doi.org/10.1080/15397730902938316.

Nguyen, K., Thai, H.T. and Vo, T. (2015), “A refined higher-order shear deformation theory for bending, vibration and buckling analysis of functionally graded sandwich plates”, *Steel Compos. Struct.*, **18**(1), 91-120. http://dx.doi.org/10.12989/scs.2015.18.1.091.

Panda, S.K. and Singh, B.N. (2013), “Thermal Postbuckling Behavior of Laminated Composite Spherical Shell Panel Using NFEM”, *Mech. Based Design Struct. Machines*, **41**(4), 468-488. https://doi.org/10.1080/15397734.2013.797330.

Poortabib, A. and Maghsoudi, M. (2014), “The analytical solution for buckling of curved sandwich beams with a transversely flexible core subjected to uniform load”, *Struct. Eng. Mech.*, **52**(2), 323-349. http://dx.doi.org/10.12989/sem.2014.52.2.323.

Reddy, J.N. (1984), “A simple higher-order shear deformation theory for laminated composite plates”, *J. Appl Mech*., **51**(4), 745-752. https://doi.org/10.1016/j.compstruct.2013.06.013.

Rizov, V., Shipsha, A. and Zenkert, D. (2005), “Indentation study of foam core sandwich composite panels”, *Compos. Struct.*, **69**(1), 95-102. https://doi.org/10.1016/j.compstruct.2004.05.013.

Seidi, J., Khalili, S.M. and Malekzadeh K. (2015), “Temperature-dependent buckling analysis of sandwich truncated conical shells with FG facesheets”, *Compos. Struct.*, **131**, 682-691. https://doi.org/10.1016/j.compstruct.2015.04.068.

Sekkal, M., Fahsi, B., Tounsi, A. and Mahmoud, S.R. (2017), “A new quasi-3D HSDT for buckling and vibration of FG plate”, *Struct. Eng. Mech.*, **64**(6), 737-749. http://dx.doi.org/10.12989/.2017.64.6.737.

Shiau, L.C. and Kuo, S.Y. (2004), “Thermal buckling of composite sandwich plates”, *Mech. Based Design Struct. Machines*, **32**(1), 57-72. https://doi.org/10.1081/SME-120026590.

Sobhy, M. (2016), “An accurate shear deformation theory for vibration and buckling of FGM sandwich plates in hygrothermal environment”, *J. Mech. Sci.*, **110**, 62-77. https://doi.org/10.1016/j.ijmecsci.2016.03.003.

Taraghi, I. and Fereidoon, A. (2016), “Non-destructive evaluation of damage modes in nanocomposite foam-core sandwich panel subjected to low-velocity impact”, *Compos. Part B Eng.*, **103**, 51-9. https://doi.org/10.1016/j.compositesb.2016.08.009.

Tounsi, A., Houari, M.S.A. and Bessaim, A. (2016), “A new 3-unknowns non-polynomial plate theory for buckling and vibration of functionally graded sandwich plate”, *Struct. Eng. Mech.*, **60**(4), 547-565. http://dx.doi.org/10.12989/sem.2016.60.4.547.

Wang, B., Wu, L., Ma, L., Sun, Y. and Du, S. (2010), “Mechanical behavior of the sandwich structures with carbon fiber-reinforced pyramidal lattice truss core”, *Materials Design (1980-2015)*, **31**(5), 2659-2563. https://doi.org/10.1016/j.matdes.2009.11.061.

Wang, X., Elishakoff, I., Qiu, Z. and Kou, C. (2011), “Non-probabilistic methods for natural frequency and buckling load of composite plate based on the experimental data”, *Mech. Based Design Struct. Machines*, **39**(1), 83-99. https://doi.org/10.1080/15397734.2011.537246.

Xin, J., Wang, J., Yao, J. and Han, Q. (2011), “Vibration, buckling and dynamic stability of a cracked cylindrical shell with time-varying rotating speed”, *Mech. Based Design Struct. Machines*, **39**(4), 461-490. https://doi.org/10.1080/15397734.2011.569301.

Yayli, M.Ö. (2018), “Buckling analysis of Euler columns embedded in an elastic medium with general elastic boundary conditions”, *Mech. Based Design Struct. Machines*, **46**(1), 110-22. https://doi.org/10.1080/15397734.2017.1292142.

PL